Title

Estimating the spatial distribution of snow water equivalent in the world's mountains

Journal

Wiley Interdisciplinary Reviews Water, 3(3)

ISSN

2049-1948

Authors

Dozier, Jeff
Bair, Edward H
Davis, Robert E

Publication Date

2016-05-01

DOI

10.1002/wat2.1140

Advanced Review

Estimating the spatial distribution of snow water equivalent in the world's mountains

Jeff Dozier,[1]* Edward H. Bair[2] and Robert E. Davis[3]

Estimating the spatial distribution of snow water equivalent (SWE) in mountainous terrain is currently the most important unsolved problem in snow hydrology. Several methods can estimate the amount of snow throughout a mountain range: (1) Spatial interpolation from surface sensors constrained by remotely sensed snow extent provides a consistent answer, with uncertainty related to extrapolation to unrepresented locations. (2) The remotely sensed date of disappearance of snow is combined with a melt calculation to reconstruct the SWE back to the last significant snowfall. (3) Passive microwave sensors offer real-time global SWE estimates but suffer from several problems like subpixel variability in the mountains. (4) A numerical model combined with assimilated surface observations produces SWE at 1-km resolution at continental scales, but depends heavily on a surface network. (5) New methods continue to be explored, for example, airborne LiDAR altimetry provides direct measurements of snow depth, which are combined with modelled snow density to estimate SWE. While the problem is aggressively addressed, the right answer remains elusive. Good characterization of the snow is necessary to make informed choices about water resources and adaptation to climate change and variability.

How to cite this article:
WIREs Water 2016, 3:461–474. doi: 10.1002/wat2.1140

INTRODUCTION

Estimating the spatial distribution of snow water equivalent (SWE) in mountainous terrain, characterized by high elevation and spatially varying topography, is currently the most important unsolved problem in snow hydrology. Worldwide, mountain snowmelt supports a billion people, and in the mountains themselves, snowmelt provides soil moisture late into the melt season. In instrumented watersheds, measurement networks provide information, but sites are on nearly flat terrain and seldom cover the highest elevations. In regions such as High Mountain Asia, the sparse surface measurement network supports neither seasonal runoff forecasts nor validation of precipitation models.

The question is, how can we estimate spatiotemporally distributed SWE in snow-dominated mountain environments, including those that lack on-the-ground measurements? Several independent methods to measure spatially distributed SWE exist, but all are problematic.

1. Two- or three-dimensional interpolation combines ground observations of SWE with maps of snow extent. Covering location and elevation and constrained by snow cover, interpolation produces a physically realistic (but not necessarily correct) value for SWE, with accuracy related to the number and distribution of ground observations.

*Correspondence to: dozier@ucsb.edu

[1]Bren School of Environmental Science & Management, University of California, Santa Barbara, CA, USA

[2]Earth Research Institute, University of California, Santa Barbara, CA, USA

[3]U.S. Army Cold Regions Research and Engineering Laboratory, Hanover, NH, USA

Conflict of interest: The authors have declared no conflicts of interest for this article.

2. The remotely sensed date of disappearance of snow from each pixel can be combined with a calculation of melt to reconstruct the accumulated SWE for each day back to the last significant snowfall. Comparison with streamflow measurements in mountain ranges where such data are available shows this method to produce enough water to supply enough runoff. Yet, SWE can only be calculated retroactively after snow disappears.
3. Passive microwave sensors offer nearly real-time global SWE estimates but suffer from several issues, notably subpixel variability in snow properties, vegetation, and terrain in the mountains owing to the large (~25 km) pixel size, signal saturation in deep snow, and SWE overestimation in the presence of large grains such as depth and surface hoar.
4. Results from the snow data assimilation system (SNODAS) are distributed from the National Snow and Ice Data Center. Similar to interpolation, SNODAS incorporates ground observations, but with a physical model that assimilates the ground and satellite observations with a numerical weather model.
5. The search for measurements of spatially distributed SWE leads to research in remote sensing, initially with airborne data. One such effort is the NASA/JPL Airborne Snow Observatory (ASO) that carries an imaging spectrometer to measure snow cover and albedo and a LiDAR altimeter to measure snow depth. Other efforts utilize active microwave sensors.

MEASUREMENT OF SNOW-COVERED AREA AND ALBEDO

Several of the methods for estimating SWE include measurements of snow extent as part of the analysis. Some studies have used snow cover duration, estimated as a byproduct of snow extent mapping, as a proxy for SWE in mountainous regions.[1]

In the solar spectrum, snow has a distinctive spectral signature—among the brightest natural substances in the visible wavelengths, reduced slightly in the near-infrared beyond 1 μm, and dark beyond about 1.6 μm in the shortwave-infrared—corresponding to the variability in the absorption properties of ice.[2,3] In the visible wavelengths, both ice and water are transparent to radiation, whereas in the shortwave-infrared both are strongly absorptive. Because snow is so distinctive, mapping of snow-covered area was one of the first applications of remote sensing in the hydrologic sciences,[4] and the combination of visible and shortwave-infrared bands enables discrimination between snow and clouds.[5] As with any remote-sensing application, a tradeoff exists between spatial and temporal resolution. Maps of snow from Landsat are available at 30 m spatial resolution,[6] but at best only every 16 days depending on cloud cover. From instruments such as MODIS (on NASA's Terra and Aqua satellites) or VIIRS (on the Suomi NPP satellite), daily snow cover at continental scales is routinely available[7–9] at 375–500 m resolution.

With a half dozen or more spectral bands covering the visible through shortwave-infrared wavelengths, it is possible to 'unmix' (separate into degenerate endmembers) pixels of 0.5 km size to estimate the fractional coverage of snow, vegetation, and soil,[10] and thereby improve the retrieval and precision of snow mapping.[11] With daily imagery available, accuracy and timeliness are improved by interpolating and smoothing across multiple days to account for cloud cover, sensor noise, and steeply off-nadir views.[12–14]

INTERPOLATION FROM GROUND-BASED SENSORS

Over much of the western United States, snow pillows measure the weight of the overlying snowpack and thereby measure the SWE. The conventional design comprises a stainless steel sandwich or a flexible impermeable membrane filled with antifreeze, and the displacement of the fluid by the snow provides the estimate of the weight. The first pillows were installed in the 1950s, but positive experience with the early installations led to their widespread adoption in the 1970s. Daily measurements from pillows are available for the western United States from the U.S. Department of Agriculture,[15] and for the Sierra Nevada from the California Department of Water Resources.[16] Problems with the pillows include bridging by frozen layers in the snowpack and accumulation and refreezing of meltwater because they impede drainage to the soil.[17,18] While other mechanisms have been tried—such as measurement of the snow's attenuation of gamma radiation from the underlying soil or the cosmos[19]—the snow pillow remains the standard method for automatic ground-based measurement of SWE. Many pillow sites also include ultrasonic depth sensors,[20] thereby allowing a calculation of mean snowpack density, along with other meteorological instruments.

As used in forecasts of the seasonal snowmelt runoff, the ground measurements provide indices of the amount of snow. The collection of pillows was not designed to estimate the actual amount of water stored in the snowpack,[21] but this situation is common in hydrologic science: we use data that were collected for operational purposes, not for science.[22] Even in regions like California's Sierra Nevada with more than 100 snow pillows, they may poorly represent the total volume of water stored in the basin's snowpack.[23] The interquartile error in the forecast of the April–July runoff is +35 to −13%, but the error distribution has long tails, both positive and negative, meaning that large over- and underestimates occur, even in years that are neither extremely dry nor wet.

Across parts of Europe[24] and north-central Asia,[25] networks of weather stations measure both precipitation and snow depth. While automated measurement of snowfall remains the subject of research, test, and evaluation,[26] many sites observe snow depth with sensors and thus have to model or manually measure snow density to arrive at point estimates of SWE.[27]

Interpolation Constrained by Remotely Sensed Snow-Covered Area

With a dense enough network of snow pillows, or other means of estimating SWE at a point location, one can spatially interpolate the SWE values in either two (Northing and Easting) or three dimensions (including elevation). Straightforward spatial interpolation, however, may spread snow well beyond the actual snow-covered area. If all the pillows are covered with snow, the interpolation method has no way to know where the SWE goes to zero. To address this artifact and to provide a realistic distribution of snow over large areas, analyses constrain the interpolation with remotely sensed maps of snow extent.[28] With enough pillows to represent location and elevation and constrained by snow cover and tapered near the snow line, interpolation produces physically realistic (but not necessarily correct) values for SWE. Figure 1(a) shows spatially distributed SWE over the Sierra Nevada on April 1, 2014, based on a three-dimensional interpolation from the snow pillows, constrained by snow-covered area.

Extrapolation into Areas not Represented by the Ground Measurements

For logistical reasons, snow pillows and other remote meteorological sites in the mountains all lie on nearly flat terrain, so they may poorly represent snow accumulation and melt rates on nearby slopes.[29] For instance, in mid-winter when all slopes nearby are covered with snow, a pillow on a valley floor may show, say, 800 mm of SWE. Yet in late spring, that pillow may show the same SWE (after more snowfall and then melt) while slopes facing more toward the sun are bare.

In addition to their not covering the slopes and aspects of the topography,[30] the highest snow pillows in many basins are 1000 m or more below the highest elevations, with the result that significant snow remains after it has melted from all the pillows (Figure 2). While forecasts based on this late-season snow apply only to a few contexts—such as a decision to generate hydropower or maintain reservoir storage—the snow at the higher elevations shows that the snow pillows underestimate some part of the spatial distribution. Historical data show that the magnitude of the orographic effect (i.e., the enhancement of precipitation with elevation) varies from year to year, depending on temperature and direction of prevailing storms and other atmospheric circulation patterns.[31]

This lack of a reliable relationship between sensors at different elevations has an important operational implication. Many snow pillows on federal land lie in designated wilderness areas, with their removal potentially mandated in the future. If they were removed, runoff forecasts would have to be based on the remaining stations, which mostly cover lower elevations. An analysis to consider the feasibility of using the measurements at lower elevations to estimate runoff showed discouraging results because of the lack of consistency with statistical relationships between the lower and higher sites.[32]

RECONSTRUCTION OF SWE FROM SNOW COVER AND MELT

Any method to measure or model the spatial distribution of snow faces the problem of independent validation. In small basins, capable skiers can carry out intensive ground surveys, the method applied in several investigations about mechanisms for snow ablation and redistribution.[33–35] With due regard for steep slopes and avalanche hazard, these studies sampled rugged terrain thoroughly during field campaigns. To extend these field methods over larger areas or longer time series is impractical, hence the need for spatially extensive analyses possible with measurements from satellites.

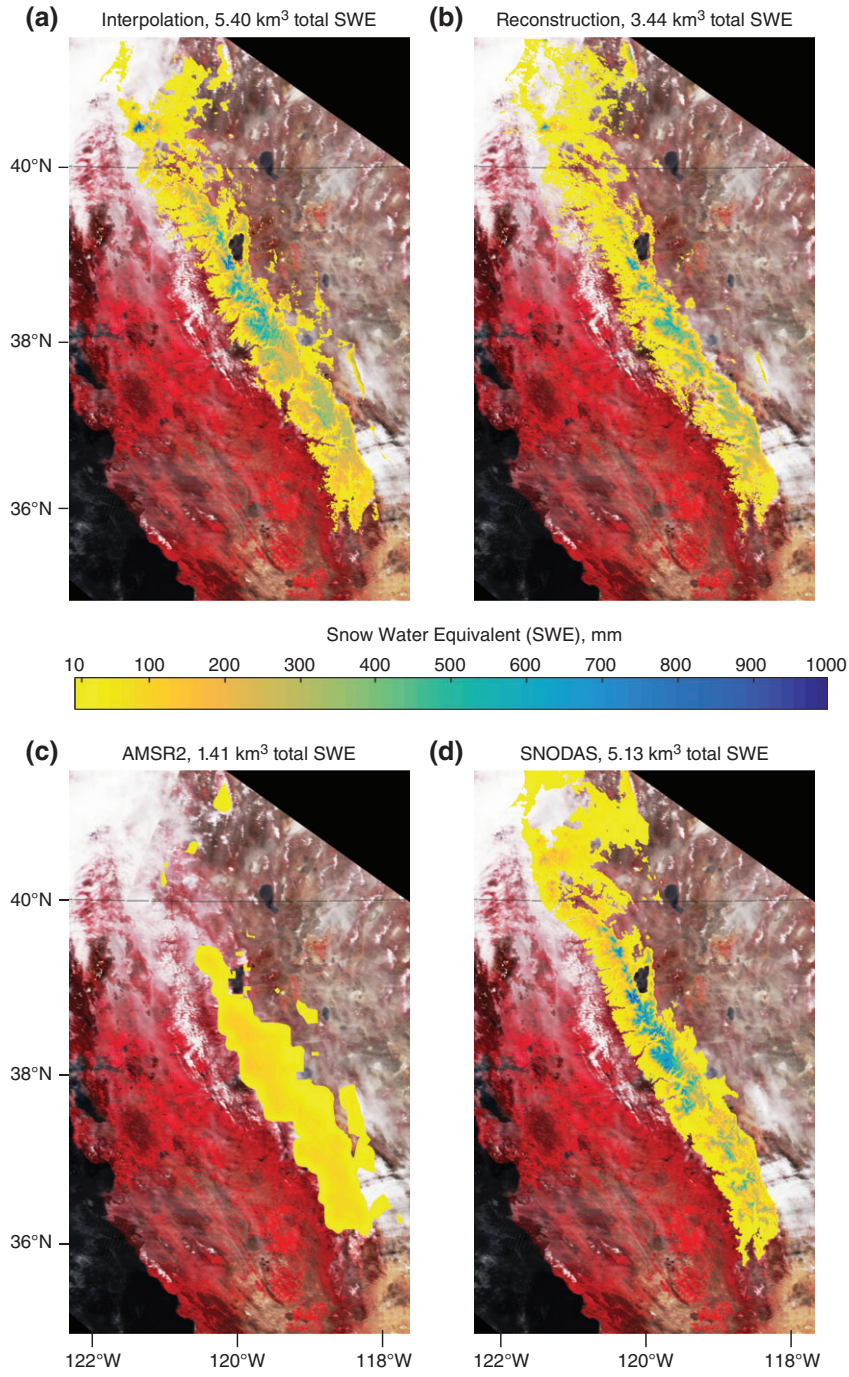

FIGURE 1 | Snow water equivalent (SWE) over the Sierra Nevada on April 1, 2014, estimated by different methods: (a) interpolation from snow pillows and satellite measurements of snow covered area; (b) reconstruction using snow-covered area from MODIS and snowmelt calculated with data from NLDAS; (c) calculated with brightness temperatures from the passive microwave sensor AMSR2; (d) modelled by the snow data assimilation system (SNODAS). The SWE images are overlaid on a MODIS image. Although clouds obscure parts of each daily MODIS image, the snow extent is interpolated and smoothed over the daily observations.[13] Images are projected at 500 m resolution.

Reconstruction by Backward Calculation after the Snow is Gone

Originally developed by Martinec and Rango,[36] the idea is simple and clever. From satellite measurements of snow-covered area, the date of disappearance of snow from each pixel is identified. Then a backward calculation of melt reconstructs the accumulated SWE for each day back to the last

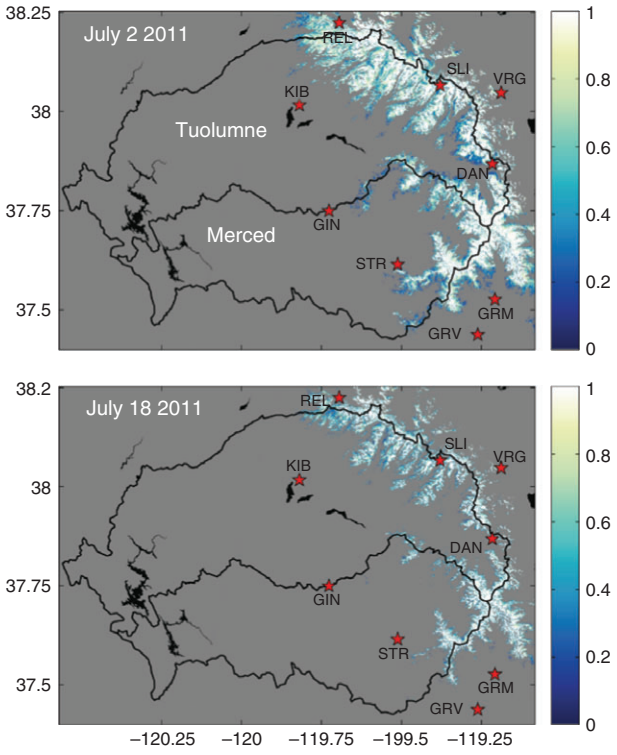

FIGURE 2 | Snow pillow locations (the red stars) superimposed on two 'July 2011' images of fractional snow cover—estimated by a spectral unmixing model[10] applied to Landsat 7 data at 30 m resolution—in the Tuolumne and Merced River basins in the Sierra Nevada, California. Significant snow remains in the basin after all pillows are bare. Table 1 lists the coordinates of the pillows and their 2011 melt-out date.

significant snowfall. During periods of no new snowfall, SWE on day N is the initial value minus the accumulated daily melt M, i.e., $\mathrm{SWE}_N = \mathrm{SWE}_0 - \sum_{d=1}^{N} M_d$. If the date when $\mathrm{SWE}_N = 0$ is identified by remote sensing, then back calculation estimates SWE every day back to day 0. Figure 1 (b) shows reconstructed SWE for the Sierra Nevada for April 1, 2014, and can be compared to Figure 1 (a). Comparison with streamflow measurements in mountain ranges where such data are available shows this method to produce enough water to supply enough runoff. At least in three seasons (2013–2015, all drier than normal), the reconstructed snow distribution compares favorably with the measurements from the ASO,[37] which uses LiDAR altimetry and a model of snow density to estimate SWE at 50 m spatial resolution. The big disadvantage of reconstruction is that SWE can only be calculated retroactively after snow disappears, and even then only back to the last significant snowfall. At best, reconstruction calculates SWE back to the seasonal peak, in areas with little accumulation during the melt season.

Variants in reconstructing the SWE include different spatial and temporal resolutions of the snow cover data, methods for estimating when the snow disappears and when peak snow occurs, and methods and data for the melt calculations. All introduce uncertainties. Landsat imagery at 30 m spatial resolution, used for validation of reconstruction in the Sierra Nevada,[38] shows clearly whether the snow has disappeared, but the 16-day orbit introduces uncertainty about when the snow disappeared. Whether the spatial or temporal resolution is most important has been a subject of contentious debate,[39,40] but this controversy may have been resolved with the use of spectral mixing models with daily MODIS data at 500-m resolution to estimate fractional snow in the pixel. In the Merced and Tuolumne River basins of the Sierra Nevada, snow depletion from reconstruction based on MODIS imagery better matches observed streamflow than interpolation utilizing snow pillow measurements.[41]

Sources of Uncertainty in Reconstruction

Because reconstruction operates only after the snow has disappeared, the SWE values cannot be used to forecast streamflow, but they do provide information about the spatial distribution of snow for studies of, for example, relationships between vegetation and snow. They also serve as a completely independent estimate of the spatial distribution of SWE for comparison with other methods or models.

The least uncertain measure is probably the pixel-specific date of snow disappearance. Cloud cover during the melt season can obscure the disappearance. In a 500 m MODIS pixel, the snow fraction will decline gradually, so the actual date at which it goes to zero is not easy to identify, but at low snow fractions the amount of snow contributes less to the reconstruction. However, reducing the incidence of falsely identified snow (false positives) is important, as incorrect identifications of persistent snow cover will add a lot of SWE to the calculation.

To estimate peak SWE, a date must be identified, and this identification is difficult from imagery alone. Maximum snow cover might not coincide with peak SWE, as maximum snow depth itself generally precedes maximum SWE because the snowpack compresses as the season progresses. In areas with snow pillows, peak SWE can be identified independently, and in such areas a blended SWE product combining the snow pillow data with reconstruction produces the most accurate match with streamflow

TABLE 1 | Locations and 2011 Melt-Out Date for the Snow Pillows in Figure 2

CDEC ID	Name	Latitude, °N	Longitude, °W	Elevation, m	2011 Melt-Out Date
DAN	Dana Meadows	37.897	119.257	2897	July 01
GIN	Gin Flat	37.767	119.773	2149	June 22
GRM	Green Mountain	37.555	119.238	2408	June 17
GRV	Graveyard Meadow	37.465	119.290	2103	June 12
KIB	Lower Kibbie Ridge	38.032	119.877	2042	June 10
REL	Lower Relief Valley	38.243	119.758	2469	July 09
SLI	Slide Canyon	38.092	119.430	2804	July 12
STR	Ostrander Lake	37.637	119.550	2499	June 30
VRG	Virginia Lakes Ridge	38.077	119.234	2835	June 20

among all methods.[42] Where there are no ground measurements, identification of the date of the peak is difficult because fluctuations in the snow cover estimate caused by daily changing viewing geometry are about as large as the true pixel-specific changes in the snow cover. However, simply back-calculating the daily melt furnishes an upper bound to the SWE accumulation.

The methods and data used to calculate melt comprise the biggest sources of uncertainty. In areas where surface micrometeorological data are available, they can be spread across topography to account for solar illumination geometry and longwave radiation.[43,44] In more extended or remote areas, products from NASA's Land Data Assimilation Systems (NLDAS in USA, GLDAS globally) provide values on solar radiation, longwave radiation, air temperature, humidity, and winds. Comparisons with surface measurements from mountain stations in the western United States show the solar radiation estimates to be reasonably accurate and without bias, longwave radiation to correspond less well with the few surface measurements available, air temperature and humidity also without bias, and surface wind poorly estimated.[45] Uncertainty also arises from the conceptual model used, which has historically included temperature-index, hybrid radiation balance with temperature index, and full energy balance.

For surfaces with high albedos, an error in the measurement of albedo leads to a greater proportional error in absorption of the solar radiation (absorption = 1 – α, so for greater values of α, a small error in α causes a greater proportional error in 1 – α). The same sensors (Landsat, MODIS, etc.) used to measure snow covered area also allow snow albedo to be estimated. Accuracies are generally good over pixels that are nearly completely covered,[46,47] but are not sufficiently validated over mixed pixels. Therefore while some efforts to reconstruct snow cover use these remotely sensed albedo estimates of the fractional snow cover, others model snow albedo based on its 'age', i.e., time since last snowfall.[42] In the mountains, snow albedo changes at different rates throughout the topography, so a model based on aging will not include the processes that cause snow to metamorphose at faster or slower rates on different exposures.[48] The accuracy and reliability of reconstruction would improve with better estimates of snow albedo from satellite.

SWE ESTIMATES FROM PASSIVE MICROWAVE SENSORS

Passive Microwave SWE Mapping

Microwave measurements of snow cover offer insensitivity to solar illumination and atmospheric conditions, which can plague optical sensors, resulting in a day-night all-weather capability. Microwave radiation emitted from the soil, expressed as brightness temperature, undergoes extinction by the overlying snow mainly through scattering, because ice is transparent over much of the microwave spectrum. Lower frequencies, typically 18–19 GHz, exhibit less extinction than a higher frequency, such as 37 GHz. Algorithms to estimate SWE primarily use multifrequency observations of the microwave emission from snow that rely on the difference in extinction properties between frequencies.[49] For example, for a sensor with bands at 18 and 37 GHz, SWE = c [T_B(18) – T_B(37)], SWE in mm and brightness temperature T_B in °K. Polarization information from these channels can also be used to differentiate shallow or deep snowpacks, adjust c for differences in layering,[50] and to detect wet snowpacks,[51] which drop the 18–37 GHz difference to nearly zero, thereby eliminating any sensitivity to SWE. Figure 1 (c) shows microwave-measured SWE over the Sierra

Nevada on April 1, 2014. The values are much smaller than those in the corresponding images in Figure 1 showing the same SWE estimated by other means.

The transfer coefficient c varies among different instruments, and is estimated from both theory and empiricism. These measurements from space date back to 1978 using a succession of sensors that were inter-calibrated[52]: the scanning multi-channel microwave radiometer (SMMR) on the Nimbus satellites, the special sensor microwave/imager (SSM/I) on the orbital platforms of the Defense Meteorological Satellite Program (DMSP), the advanced microwave scanning radiometer (AMSR-E) on NASA's EOS Aqua spacecraft from 2002 to 2011, AMSR2 on JAXA's GCOM-W1 spacecraft since 2012, and the Chinese FengYung series starting in 2008.

The low-energy levels of microwave emission at Earth surface temperatures require coarse resolutions, larger pixels of tens of kilometers, to collect enough energy to achieve the precision and accuracy needed for the observations. This has the effect of mixing snow with different properties over different land covers with a variety of terrain configurations into one set of brightness temperatures per pixel with which to feed retrieval algorithms.[50] Accordingly, nearly all retrieval algorithms rely on empirical or model-derived coefficients, optimized to account for the variable frequency and polarization effects of SWE under different conditions.[51] These algorithms have performed best over regions with consistent snow properties and land cover types, thin forests, and little topographic variability. Examples include the boreal forest as it transitions to tundra,[53] the northern Great Plains,[54] and much of the continental United States except for the mountains.[55] Some evidence suggests that regionally calibrated algorithms improve retrieval performance, but this approach suffers from the lack of suitable calibration data in many mountain ranges.

Sources of Uncertainty in Passive Microwave Remote Sensing of Snow

Differences in snow properties affect microwave extinction. Coarser texture with larger grain sizes increases the scattering component of extinction. For coarse snow, global microwave retrievals tend to overestimate total SWE.[56,57] Internal reflections and larger effective grain size manifested by stratigraphy and ice lenses have similar effects.[58,59] Total snow depth and SWE also affect the degree to which the observations can differentiate SWE based on frequency gradients; at SWE greater than 150–200 mm the frequency difference vanishes,[60–63] and as SWE increases above that value the brightness temperatures rise again because of emission from the deep snowpack itself. Because water is about 80× as absorptive as ice across the microwave spectrum, liquid water in the snowpack increases the microwave emission, making the signal from snow similar to that from wet soil.[64] As snow generally becomes wet from the top down, the emission from the ground becomes obscured and the brightness temperatures represent emission from near the wet snow surface.[65]

Land cover type, notably forest, adversely affects microwave retrieval of snow properties.[53,66] Viewed from above, a forest consists of a canopy fraction and a gap fraction, both between crowns and through crowns. From the viewing angle of a passive sensor, microwave retrievals depend on the viewable gap fraction, from which snow contributes to the observation, and emission and scattering properties of the crowns. With increasing viewing angle off-nadir, viewable gaps decrease,[67] and tree crowns generally have a warmer brightness temperature than the underlying snow.[68] By increasing radiometric brightness across frequencies, forest cover produces an underestimate of SWE with the standard algorithms, as it diminishes the brightness temperature difference of snow between frequencies. On the other hand, the issue does not appear quite so neatly resolved in observations. Some studies have shown improved correlation between modelled SWE and microwave retrievals with increasing forest cover to about 30% or 40%,[63] while others show better correlation at lower fractions.[55]

SNOW DATA ASSIMILATION SYSTEM

SNODAS, the Snow Data Assimilation System run operationally by the U.S. National Snow and Ice Data Center (NSIDC), was developed at the NOAA National Weather Service office in Chanhassen, MN. SNODAS ingests a variety of datasets daily, including meteorological data, ground-based SWE, and snow depth from stations operated by a range of U.S. federal and state agencies and Canadian provincial agencies. In all, SNODAS uses meteorological data from 100,000 stations and snow information from 40,000 locations. Remotely sensed data ingested include snow-covered area from MODIS and 1500–2500 airborne gamma radiation estimates of SWE (a method that is used mostly in the Great Plains, and thus not covered in this review). Combined with the observations, SNODAS ingests

downscaled weather modelling results and combines them with an energy and mass balance snow model. The SNODAS scheme includes methods to assimilate remotely sensed snow extent and ground station data, to produce estimated SWE daily at 1-km resolution at hourly time steps. Analysts determine whether to assimilate ground measurements, through nudging or adoption, based on local knowledge of the grid cells coinciding with the observations. They consider whether deviations show spatial coherence. SNODAS thus performs functions akin to remote-sensing aided interpolation, but uses a physical basis and weather models rather than just geostatistical interpolation.

Especially in mountainous regions, SNODAS depends on observations to assimilate. In the US Rocky Mountains, it explained 30% of the variance in observed SWE, without empirical adjustments accounting for wind redistribution, vegetation, and terrain.[69]

COMPARISON BETWEEN INTERPOLATION, RECONSTRUCTION, PASSIVE MICROWAVE, AND SNODAS

Interpolation, reconstruction, and SNODAS rely heavily on the same or similar satellite-based snow-covered area estimates based on visible through near-infrared bands. Thus, these methods tend to show snow in the same areas, but with differing SWE. Interpolation and SNODAS produce similar SWE estimates near pillows over most of the Sierra Nevada (Figure 1(a) and (d)), but they differ greatly when extrapolating to areas without pillows or in areas above the highest elevations, such as the White Mountains (37.649°N 118.251°W) or the upper elevations on Mt. Shasta (41.409°N, 122.197°W). For comparison, reconstruction (Figure 3(a)–(c)) estimates more than two times the SWE on the upper elevations of Mt. Shasta compared to interpolation and more than three times compared to SNODAS. Moreover, both interpolation and especially SNODAS miss the huge accumulation of snow at Mt. Shasta's higher elevations (Figure 3(d) and (e)) because the only snow pillow in the area lies at 2060 m elevation, more than 2000 below the 4322 m summit. Given that Mt. Shasta contains numerous permanent snowfields and the largest glaciers in California, we suggest that the reconstructed estimates are more realistic for this area, yet there are no accurate spatial SWE measurements that can be treated as ground truth for verification. Interpolation and SNODAS produce more total SWE volume (5.40 and 5.13 km^3) than reconstruction (3.44 km^3) while AMSR2 estimates much less (1.41 km^3). Preliminary comparisons with ASO suggest that SNODAS may overestimate SWE in spring,[70] possibly because of a reliance on snow pillow measurements, which late in the season can hold more SWE than the average of the nearby surrounding terrain because they impede drainage to the underlying soil.[18]

In contrast to these three methods, which all show over 1000 mm of SWE in some areas even though the Sierra-wide SWE on April 1, 2014 totaled only 35% of that date's average SWE, AMSR2 shows a SWE maximum of only 139 mm. Likewise, AMSR2 shows much less SWE volume overall (1.49 km^3). These differences can be explained by the decrease in the frequency difference as the SWE rises toward 150 mm and the large 10 km pixels of AMR2. In relative terms, AMSR2 correctly identifies areas in the central Sierra Nevada as having the most SWE and picks up the general NW to SE orientation of the mountain range and its snowpack. Perhaps the most important feature of AMSR2 is that its data are independent of the other methods; AMSR2 does not rely on snow-covered area estimates of the other three methods, which can suffer from snow/cloud discrimination problems, especially for thin clouds.

RESEARCH EFFORTS TO IMPROVE THE MEASUREMENT OF SWE IN THE MOUNTAINS

Airborne Snow Observatory

The search for measurements of spatially distributed SWE leads to research in remote sensing, initially with airborne data. One such effort is the NASA/JPL ASO that carries an imaging spectrometer to measure snow cover and albedo and a LiDAR altimeter to measure snow depth by subtracting the elevation of bare ground, measured during summer, from the elevation of the top of the snowpack.[37] Combining depth with modelled density yields SWE, but at this time the airborne mission covers only a few drainage basins in California's Sierra Nevada and the Colorado Rockies.

Unmanned Aerial Vehicles

Unmanned Aerial Vehicles (UAVs) have been used to map snow depth in complex terrain using stereo pairs and photogrammetry[71,72] with RMSE values of 10–30 cm. As with the ASO data, modeled snow densities can be combined with these depth

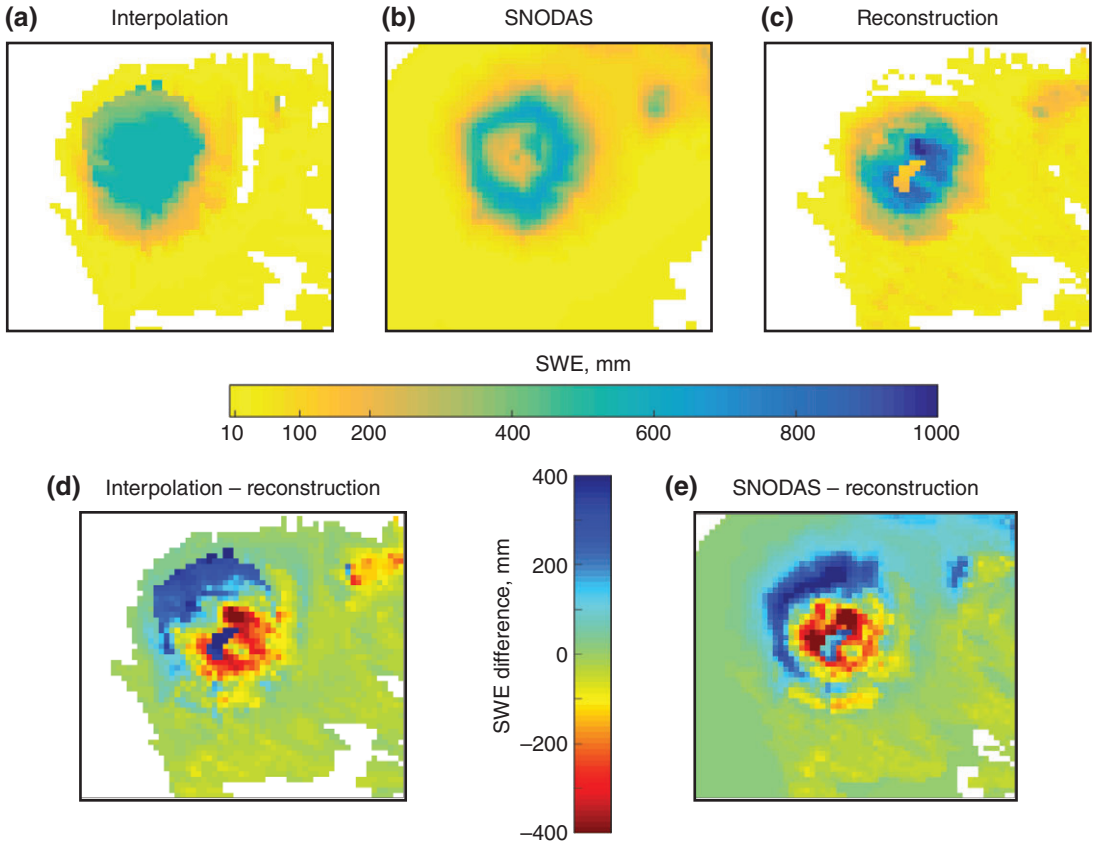

FIGURE 3 | Comparison of three methods to estimate snow water equivalent (SWE) on Mt. Shasta, California, on April 1, 2014, in a small area within a small region (28 × 30 km) that Figure 1 covers. The top row identifies the SWE values: (a) interpolation; (b) snow data assimilation system (SNODAS); and (c) reconstruction. The bottom row identifies the differences: (d) interpolation minus reconstruction; and (e) SNODAS minus reconstruction.

measurements to estimate SWE. Current regulations in the United States and other countries make UAV operation for research difficult and limit operation to line-of-sight, but these regulations are evolving. Small UAVs also suffer from limited flight time, typically around 30 min. Restrictions imposed by the line-of-sight and flight time severely limit aerial coverage. Recently, UAVs have been developed that carry compact LiDARs and hyperspectral cameras, potentially offering similar snow mapping capabilities as the ASO. Because of their ability to fly close to their targets, such UAV LiDARs have advertised RMSE values down to 0.1 cm.

Active Microwave Remote Sensing

Active microwave remote sensing (radar) of SWE can acquire observations at much finer resolution than can passive microwave retrievals because an active system provides its own illumination. Spaceborne systems—such as the European Remote-sensing Satellites-1 and -2 (ERS-1 and ERS-2), RADARSAT-1 and RADARSAT-2, and Envisat SAR instruments—have resolutions as fine as 30 m. Like passive microwave observation of snow, approaches differentiate the signal from the underlying ground and the signal that manifests the properties of the snow. The retrievals employ a frequency and polarizations that penetrate snow, and those that the snow scatters or absorbs.

These techniques rely on quantifying microwave backscatter from the snow surface, the snow volume, and the ground. Making these measurements most useful also requires corrections for terrain and vegetation, because the topographic geometry exerts a strong control on the backscatter energy, and vegetation introduces additional scattering processes. The spaceborne systems mentioned in the paragraph above all provide just one frequency, and thus have not proved successful in estimating SWE. Results

from the SIR-C/X-SAR mission proved encouraging,[73–75] but that mission comprised just two ten-day flights. Accordingly, recent concepts for satellite missions include a dual-frequency approach, possibly combined with a passive sensor, as recommended by the U.S. National Academy of Sciences' 'decadal survey' for Earth scence.[76] Such missions have been proposed and designed—CoReH$_2$O to the European Space Agency[77] and SCLP (snow and cold land processes) to NASA—but neither was selected for flight. NASA supports an international working group examining future options and intermediate steps for a spaceborne sensor that can measure SWE and other snow properties (Box 1).[78]

CONCLUSION

In regions like the mountainous western United States where snowfall constitutes a significant fraction of total precipitation, the snowpack delays the resulting runoff into the time of year where water demand is greater, so measurement of snow on the ground has been an important component of hydrologic forecasting for a century.[82] Measurements at a set of local sites suffer from the lack of representation of the topographic setting, so while statistically they can estimate the volume of water stored as snow, those estimates occasionally have large errors. In regions like High Mountain Asia with an austere surface infrastructure, an adequately dense surface network is not available. In both types of regions, therefore, actual estimates of the spatial distribution of SWE would provide insight about sources of error in forecasts and address effects of snow distribution in mountain ecosystems.

Several independent methods produce estimates of the spatial distribution of snow, but all are problematic in some ways. Interpolation requires a surface network, which often does not cover the highest elevations. Reconstruction does not cover the accumulation part of the snow season, and estimates are available only after the snow is gone. Passive microwave sensors provide good information on thin, cold snow in areas of simple topography but suffer from several artifacts in mountains terrain and generally underestimate the SWE. Numerical weather models, like those used in SNODAS, are too coarse to simulate many snowfall and redistribution processes and often do not correctly calculate the orographic enhancement of precipitation or subsequent melt. Among all the uses of remote sensing in hydrology, SWE is the one where new innovations would deliver the greatest benefit.

BOX 1

INTERANNUAL PERSISTENCE OF SPATIAL PATTERNS

Snow loading in mountainous areas tends to repeat, pattern-wise, as SWE builds up, integrating snowfall and redistribution over many storms followed by spring melt.[79–81] Here we have described approaches observing snow cover duration and the contemporaneous energy budget, which provide estimates of SWE, and other indices of SWE from interpolation and modelling from remote sensing and observations at point-like locations in the mountains. We have not addressed possibilities and potential of long-term time series of this information. As years progress, the documented themes and variations of SWE accumulation and depletion expand to encompass more and more interannual and inter-basin variability. The large resulting datasets may yield new understanding of the climatic response of terrain units. By establishing geospatial priors, antecedent indicators may allow us to understand SWE in mountains independently through continuous efforts of interpolating and modelling the remotely sensed updates.

FURTHER READING

Armstrong P. *The Log of a Snow Survey: Skiing and Working in a Mountain Winter World*. Bloomington, IN: Abbott Press; 2014.

Dozier J. Mountain hydrology, snow color, and the fourth paradigm. *Eos Trans Am Geophys Union* 2011, 92:373–375. doi:10.1029/2011EO430001.

REFERENCES

1. Dedieu JP, Lessard-Fontaine A, Ravazzani G, Cremonese E, Shalpykova G, Beniston M. Shifting mountain snow patterns in a changing climate from remote sensing retrieval. *Sci Total Environ* 2014, 493:1267–1279. doi:10.1016/j.scitotenv.2014.04.078.
2. Warren SG. Optical properties of snow. *Rev Geophys* 1982, 20:67–89. doi:10.1029/RG020i001p00067.
3. Warren SG, Brandt RE. Optical constants of ice from the ultraviolet to the microwave: a revised compilation. *J Geophys Res* 2008, 113:D14220. doi:10.1029/2007JD009744.
4. Lettenmaier DP, Alsdorf D, Dozier J, Huffman GJ, Pan M, Wood EF. Inroads of remote sensing into hydrologic science during the WRR era. *Water Resour Res* 2015, 51:7309–7342. doi:10.1002/2015WR017616.
5. Crane RG, Anderson MR. Satellite discrimination of snow/cloud surfaces. *Int J Remote Sens* 1984, 5:213–223. doi:10.1080/01431168408948799.
6. Dozier J. Spectral signature of alpine snow cover from the Landsat Thematic Mapper. *Remote Sens Environ* 1989, 28:9–22. doi:10.1016/0034-4257(89)90101-6.
7. Hall DK, Riggs GA, Salomonson VV, DiGirolamo NE, Bayr KJ. MODIS snow-cover products. *Remote Sens Environ* 2002, 83:181–194. doi:10.1016/S0034-4257(02)00095-0.
8. Reba ML, Marks D, Seyfried M, Winstral A, Kumar M, Flerchinger G. A long-term data set for hydrologic modeling in a snow-dominated mountain catchment. *Water Resour Res* 2011, 47:W07702. doi:10.1029/2010WR010030.
9. Garen DC, Johnson GL, Hanson CL. Mean areal precipitation for daily hydrologic modeling in mountainous regions. *J Am Water Resour Assoc* 1994, 30:481–491. doi:10.1111/j.1752-1688.1994.tb03307.x.
10. Painter TH, Rittger K, McKenzie C, Slaughter P, Davis RE, Dozier J. Retrieval of subpixel snow-covered area, grain size, and albedo from MODIS. *Remote Sens Environ* 2009, 113:868–879. doi:10.1016/j.rse.2009.01.001.
11. Rittger K, Painter TH, Dozier J. Assessment of methods for mapping snow cover from MODIS. *Adv Water Resour* 2013, 51:367–380. doi:10.1016/j.advwatres.2012.03.002.
12. Cline DW, Carroll TR. Inference of snow cover beneath obscuring clouds using optical remote sensing and a distributed snow energy and mass balance model. *J Geophys Res* 1999, 104:19631–19644. doi:10.1029/1999jd900249.
13. Dozier J, Painter TH, Rittger K, Frew JE. Time-space continuity of daily maps of fractional snow cover and albedo from MODIS. *Adv Water Resour* 2008, 31:1515–1526. doi:10.1016/j.advwatres.2008.08.011.
14. Molotch NP, Fassnacht SR, Bales RC, Helfrich SR. Estimating the distribution of snow water equivalent and snow extent beneath cloud cover in the Salt–Verde River basin, Arizona. *Hydrol Process* 2004, 18:1595–1611. doi:10.1002/hyp.1408.
15. Daly C, Neilson RP, Phillips DL. A statistical-topographic model for mapping climatological precipitation over mountainous terrain. *J Appl Meteorol* 1994, 33:140–158. doi:10.1175/1520-0450(1994)033<0140:ASTMFM>2.0.CO;2.
16. Marks D, Winstral A, Reba M, Pomeroy J, Kumar M. An evaluation of methods for determining during-storm precipitation phase and the rain/snow transition elevation at the surface in a mountain basin. *Adv Water Resour* 2013, 55:98–110. doi:10.1016/j.advwatres.2012.11.012.
17. Cox LM, Bartee D, Crook A, Farnes PE, Smith JL. The care and feeding of snow pillows. In: *Proceedings of the 46th Annual Western Snow Conference*, Otter Rock, OR, 1978, 40–47.
18. Johnson JB, Marks D. The detection and correction of snow water equivalent pressure sensor errors. *Hydrol Process* 2004, 18:3513–3525. doi:10.1002/hyp.5795.
19. Osterhuber RJ, Gehrke F, Condreva K. Snowpack snow water equivalent measurement using the attenuation of cosmic gamma radiation. In: *Proceedings of the 66th Annual Western Snow Conference*, Snowbird, UT, 1998, 59–62.
20. Ryan WA, Doesken NJ, Fassnacht SR. Evaluation of ultrasonic snow depth sensors for U.S. snow measurements. *J Atmos Oceanic Tech* 2008, 25:667–684. doi:10.1175/2007JTECHA947.1.
21. Daly SF, Davis R, Ochs E, Pangburn T. An approach to spatially distributed snow modelling of the Sacramento and San Joaquin basins, California. *Hydrol Process* 2000, 14:3257–3271. doi:10.1002/1099-1085(20001230)14:18<3257::AID-HYP199>3.0.CO;2-Z.
22. Dozier J. Opportunities to improve hydrologic data. *Rev Geophys* 1992, 30:315–331. doi:10.1029/92RG01440.
23. Bales RC, Molotch NP, Painter TH, Dettinger MD, Rice R, Dozier J. Mountain hydrology of the western United States. *Water Resour Res* 2006, 42:W08432. doi:10.1029/2005WR004387.
24. Klok EJ, Klein Tank AMG. Updated and extended European dataset of daily climate observations. *Int J Climatol* 2009, 29:1182–1191. doi:10.1002/joc.1779.
25. Schöne T, Zech C, Unger-Shayesteh K, Rudenko V, Thoss H, Wetzel HU, Gafurov A, Illigner J, Zubovich A. A new permanent multi-parameter monitoring network in Central Asian high mountains—from measurements to data bases. *Geosci Instrum Method Data Syst* 2013, 2:97–111. doi:10.5194/gi-2-97-2013.

26. Rasmussen R, Baker B, Kochendorfer J, Meyers T, Landolt S, Fischer AP, Black J, Thériault JM, Kucera P, Gochis D, et al. How well are we measuring snow: the NOAA/FAA/NCAR winter precipitation test bed. *Bull Am Meteorol Soc* 2011, 93:811–829. doi:10.1175/BAMS-D-11-00052.1.

27. Jonas T, Marty C, Magnusson J. Estimating the snow water equivalent from snow depth measurements in the Swiss Alps. *J Hydrol* 2009, 378:161–167. doi:10.1016/j.jhydrol.2009.09.021.

28. Fassnacht SR, Dressler KA, Bales RC. Snow water equivalent interpolation for the Colorado River Basin from snow telemetry (SNOTEL) data. *Water Resour Res* 2003, 39:1208. doi:10.1029/2002WR001512.

29. Meromy L, Molotch NP, Link TE, Fassnacht SR, Rice R. Subgrid variability of snow water equivalent at operational snow stations in the western USA. *Hydrol Process* 2013, 27:2383–2400. doi:10.1002/hyp.9355.

30. Fassnacht SR, Dressler KA, Hultstrand DM, Bales RC, Patterson G. Temporal inconsistencies in coarse-scale snow water equivalent patterns: Colorado River Basin snow telemetry-topography regressions. *Pirineos* 2012, 167:165–185. doi:10.3989/Pirineos.2012.167008.

31. Lundquist JD, Minder J, Neiman PJ, Sukovich E. Relationships between barrier jet heights, orographic precipitation gradients, and streamflow in the northern Sierra Nevada. *J Hydrometeorol* 2010, 11:1141–1156. doi:10.1175/2010JHM1264.1.

32. McGurk BJ, Edens TJ, Azuma DL. Predicting wilderness snow water equivalent with nonwilderness snow sensors. *J Am Water Resour Assoc* 1993, 29:85–94. doi:10.1111/j.1752-1688.1993.tb01506.x.

33. Elder K, Dozier J, Michaelsen J. Snow accumulation and distribution in an alpine watershed. *Water Resour Res* 1991, 27:1541–1552. doi:10.1029/91WR00506.

34. Winstral A, Elder K, Davis RE. Spatial snow modeling of wind-redistributed snow using terrain-based parameters. *J Hydrometeorol* 2002, 3:524–538. doi:10.1175/1525-7541(2002)003<0524:SSMOWR>2.0.CO;2.

35. Musselman KN, Molotch NP, Brooks PD. Effects of vegetation on snow accumulation and ablation in a mid-latitude sub-alpine forest. *Hydrol Process* 2008, 22:2767–2776. doi:10.1002/hyp.7050.

36. Martinec J, Rango A. Areal distribution of snow water equivalent evaluated by snow cover monitoring. *Water Resour Res* 1981, 17:1480–1488. doi:10.1029/WR017i005p01480.

37. McGurk BJ, Painter TH. Airborne Snow Observatory: next generation of basin snow measurement, modeling, and forecasting. In: *Proceedings of 81st Annual Western Snow Conference*, Jackson Hole, WY, 2013, 43–52.

38. Cline DW, Bales RC, Dozier J. Estimating the spatial distribution of snow in mountain basins using remote sensing and energy balance modeling. *Water Resour Res* 1998, 34:1275–1285. doi:10.1029/97WR03755.

39. Molotch NP, Margulis SA. Estimating the distribution of snow water equivalent using remotely sensed snow cover data and a spatially distributed snowmelt model: a multi-resolution, multi-sensor comparison. *Adv Water Resour* 2008, 31:1503–1514. doi:10.1016/j.advwatres.2008.07.017.

40. Slater AG, Clark MP, Barrett AP. Comment on "Estimating the distribution of snow water equivalent using remotely sensed snow cover data and a spatially distributed snowmelt model …". *Adv Water Resour* 2009, 32:1680–1684. doi:10.1016/j.advwatres.2009.09.001.

41. Rice R, Bales RC, Painter TH, Dozier J. Snow water equivalent along elevation gradients in the Merced and Tuolumne River basins of the Sierra Nevada. *Water Resour Res* 2011, 47:W08515. doi:10.1029/2010wr009278.

42. Guan B, Molotch NP, Waliser DE, Jepsen SM, Painter TH, Dozier J. Snow water equivalent in the Sierra Nevada: blending snow sensor observations with snowmelt model simulations. *Water Resour Res* 2013, 49:5029–5046. doi:10.1002/wrcr.20387.

43. Dozier J, Frew J. Rapid calculation of terrain parameters for radiation modeling from digital elevation data. *IEEE Trans Geosci Remote Sens* 1990, 28:963–969. doi:10.1109/36.58986.

44. Kahl A, Winstral A, Marks D, Dozier J. Using satellite imagery and the distributed Isnobal energy balance model to derive SWE heterogeneity in mountainous basins. In: Pomeroy JW, Whitfield PH, Spence C, eds. *Putting Prediction in Ungauged Basins into Practice*. Ottawa: Canadian Water Resources Association; 2014, 243–253.

45. Rittger KE. Spatial estimates of snow water equivalent in the Sierra Nevada. PhD Thesis, University of California, Santa Barbara, CA, 2012.

46. Stroeve J, Box JE, Gao F, Liang S, Nolin A, Schaaf C. Accuracy assessment of the MODIS 16-day albedo product for snow: comparisons with Greenland in situ measurements. *Remote Sens Environ* 2005, 94:46–60. doi:10.1016/j.rse.2004.1009.1001.

47. Wang Z, Schaaf CB, Strahler AH, Chopping MJ, Román MO, Shuai Y, Woodcock CE, Hollinger DY, Fitzjarrald DR. Evaluation of MODIS albedo product (MCD43A) over grassland, agriculture and forest surface types during dormant and snow-covered periods. *Remote Sens Environ* 2014, 140:60–77. doi:10.1016/j.rse.2013.08.025.

48. Molotch NP, Painter TH, Bales RC, Dozier J. Incorporating remotely-sensed snow albedo into a spatially-distributed snowmelt model. *Geophys Res Lett* 2004, 31:L03501. doi:10.1029/2003GL019063.

49. Chang ATC, Foster JL, Hall DK. Nimbus-7 SMMR derived global snow cover parameters. *Ann Glaciol* 1987, 9:39–44.
50. Vander Jagt BJ, Durand MT, Margulis SA, Kim EJ, Molotch NP. The effect of spatial variability on the sensitivity of passive microwave measurements to snow water equivalent. *Remote Sens Environ* 2013, 136:163–179. doi:10.1016/j.rse.2013.05.002.
51. Clifford D. Global estimates of snow water equivalent from passive microwave instruments: history, challenges and future developments. *Int J Remote Sens* 2010, 31:3707–3726. doi:10.1080/01431161.2010.483482.
52. Shi J, Xiong C, Jiang L. Review of snow water equivalent microwave remote sensing. *Sci China Earth Sci* 2016, 59:1–15. doi:10.1007/s11430-015-5225-0.
53. Derksen C, Walker A, Goodison B. Evaluation of passive microwave snow water equivalent retrievals across the boreal forest/tundra transition of western Canada. *Remote Sens Environ* 2005, 96:315–327. doi:10.1016/j.rse.2005.02.014.
54. Mote TL, Grundstein AJ, Leathers DJ, Robinson DA. A comparison of modeled, remotely sensed, and measured snow water equivalent in the northern Great Plains. *Water Resour Res* 2003, 39:1209. doi:10.1029/2002WR001782.
55. Vuyovich CM, Jacobs JM, Daly SF. Comparison of passive microwave and modeled estimates of total watershed SWE in the continental United States. *Water Resour Res* 2014, 50:9088–9102. doi:10.1002/2013WR014734.
56. Foster JL, Hall DK, Chang ATC, Rango A, Wergin W, Erbe E. Effects of snow crystal shape on the scattering of passive microwave radiation. *IEEE Trans Geosci Remote Sens* 1999, 37:1165–1168. doi:10.1109/36.752235.
57. Josberger EG, Mognard NM. A passive microwave snow depth algorithm with a proxy for snow metamorphism. *Hydrol Process* 2002, 16:1557–1568. doi:10.1002/hyp.1020.
58. Durand M, Kim EJ, Margulis SA, Molotch NP. A first-order characterization of errors from neglecting stratigraphy in forward and inverse passive microwave modeling of snow. *IEEE Geosci Remote Sens Lett* 2011, 8:730–734. doi:10.1109/LGRS.2011.2105243.
59. Wiesmann A, Mätzler C. Microwave emission model of layered snowpacks. *Remote Sens Environ* 1999, 70:307–316. doi:10.1016/S0034-4257(99)00046-2.
60. Hancock S, Baxter R, Evans J, Huntley B. Evaluating global snow water equivalent products for testing land surface models. *Remote Sens Environ* 2013, 128:107–117. doi:10.1016/j.rse.2012.10.004.
61. Kelly R. The AMSR-E snow depth algorithm: description and initial results. *J Remote Sens Soc Japan* 2009, 29:307–317. doi:10.11440/rssj.29.307.
62. Takala M, Luojus K, Pulliainen J, Derksen C, Lemmetyinen J, Kärnä J-P, Koskinen J, Bojkov B. Estimating northern hemisphere snow water equivalent for climate research through assimilation of space-borne radiometer data and ground-based measurements. *Remote Sens Environ* 2011, 115:3517–3529. doi:10.1016/j.rse.2011.08.014.
63. Tedesco M, Narvekar PS. Assessment of the NASA AMSR-E SWE product. *IEEE JSTARS* 2010, 3:141–159. doi:10.1109/JSTARS.2010.2040462.
64. Mätzler C. Applications of the interaction of microwaves with the natural snow cover. *Remote Sens Rev* 1987, 2:259–387. doi:10.1080/02757258709532086.
65. Hallikainen MT, Ulaby F, Abdelrazik M. Dielectric properties of snow in the 3 to 37 GHz range. *IEEE Trans Antenn Propag* 1986, 34:1329–1340. doi:10.1109/TAP.1986.1143757.
66. Foster JL, Sun C, Walker JP, Kelly REJ, Chang ATC, Dong J, Powell H. Quantifying the uncertainty in passive microwave snow water equivalent observations. *Remote Sens Environ* 2005, 94:187–203. doi:10.1016/j.rse.2004.09.012.
67. Liu J, Melloh RA, Woodcock CE, Davis RE, Ochs ES. The effect of viewing geometry and topography on viewable gap fractions through forest canopies. *Hydrol Process* 2004, 18:3595–3607. doi:10.1002/hyp.5802.
68. Pulliainen J, Hallikainen M. Retrieval of regional snow water equivalent from space-borne passive microwave observations. *Remote Sens Environ* 2001, 75:76–85. doi:10.1016/S0034-4257(00)00157-7.
69. Clow DW, Nanus L, Verdin KL, Schmidt J. Evaluation of SNODAS snow depth and snow water equivalent estimates for the Colorado Rocky Mountains, USA. *Hydrol Process* 2012, 26:2583–2591. doi:10.1002/hyp.9385.
70. Bair EH, Rittger K, Dozier J, Davis RE. Comparison and error analysis of reconstructed SWE to Airborne Snow Observatory measurements in the Upper Tuolumne Basin, CA. In: *Proceedings of Western Snow Conference* 2015, Grass Valley, CA, in press.
71. Vander Jagt B, Lucieer A, Wallace L, Turner D, Durand M. Snow depth retrieval with UAS using photogrammetric techniques. *Geosciences* 2015, 5:264–285. doi:10.3390/geosciences5030264.
72. Bühler Y, Marty M, Egli L, Veitinger J, Jonas T, Thee P, Ginzler C. Snow depth mapping in high-alpine catchments using digital photogrammetry. *The Cryosphere* 2015, 9:229–243. doi:10.5194/tc-9-229-2015.
73. Shi J, Dozier J. Estimation of snow water equivalence using SIR-C/X-SAR, Part I: Inferring snow density and subsurface properties. *IEEE Trans Geosci Remote Sens* 2000, 38:2465–2474. doi:10.1109/36.885195.
74. Shi J, Dozier J. Estimation of snow water equivalence using SIR-C/X-SAR, Part II: inferring snow depth and grain size. *IEEE Trans Geosci Remote Sens* 2000, 38:2475–2488. doi:10.1109/36.885196.

75. Shi J, Dozier J. Mapping seasonal snow with SIR-C/X-SAR in mountainous areas. *Remote Sens Environ* 1997, 59:294–307. doi:10.1016/S0034-4257(96)00146-0.

76. National Research Council. *Earth Science and Applications from Space: National Imperatives for the Next Decade and Beyond*. Washington, DC: National Academies Press; 2007.

77. Rott H, Yueh SH, Cline DW, Duguay C, Essery R, Haas C, Heliere F, Kern M, Macelloni G, Malnes E, et al. Cold regions hydrology high-resolution observatory for snow and cold land processes. *Proc IEEE* 2010, 98:752–765. doi:10.1109/jproc.2009.2038947.

78. Church JE. Snow surveying: its principles and possibilities. *Geog Rev* 1933, 23:529–563. doi:10.2307/209242.

79. Erickson TA, Williams MW, Winstral A. Persistence of topographic controls on the spatial distribution of snow in rugged mountain terrain, Colorado, United States. *Water Resour Res* 2005, 41:W04014. doi:04010.01029/02003WR002973.

80. Deems JS, Fassnacht SR, Elder KJ. Interannual consistency in fractal snow depth patterns at two Colorado mountain sites. *J Hydrometeorol* 2008, 9:977–988. doi:10.1175/2008JHM901.1.

81. Schirmer M, Wirz V, Clifton A, Lehning M. Persistence in intra-annual snow depth distribution: 1. measurements and topographic control. *Water Resour Res* 2011, 47:W09516. doi:10.1029/2010WR009426.

82. Church JE. Recent studies of snow in the United States. *Q J R Meteorol Soc* 1914, 40:43–52. doi:10.1002/qj.49704016905.

